

Parathyroid Imaging with Technetium-99m-Sestamibi: Preoperative Localization and Tissue Uptake Studies

Michael J. O'Doherty, Andrew G. Kettle, Philip Wells, Richard E.C. Collins, and Anthony J. Coakley

Departments of Nuclear Medicine and Surgery, Kent and Canterbury Hospital, Canterbury, Kent, United Kingdom

The accepted radionuclide method for imaging abnormal parathyroid tissue has been the combined use of [^{99m}Tc]pertechnetate ^{201}Tl -chloride. Various problems with this approach, however, have suggested the need for an improved parathyroid imaging agent. This study examined the use of ^{99m}Tc -sestamibi as a parathyroid imaging agent compared with ^{201}Tl -chloride. Fifty-seven patients were scanned with both ^{99m}Tc -sestamibi and ^{201}Tl preoperatively. There were 40 adenomas, of which 37 were localized with ^{201}Tl and 39 with sestamibi. Fifteen patients had hyperplastic glands, of which 29 glands were localized with ^{201}Tl and 32 with sestamibi. Possible differences in uptake of the two agents by thyroid and parathyroid tissue were examined by administering 10 MBq of each agent to patients undergoing surgical exploration and biopsy. Preoperatively 20 patients were studied (13 adenomas and 7 with hyperplasia). Thallium-201 uptake was higher in both the parathyroid and thyroid tissue than sestamibi. However, the uptake per gram of parathyroid tissue of sestamibi was higher than the uptake per gram of thyroid tissue. This was not true for ^{201}Tl . Technetium-99m-sestamibi was at least as effective as ^{201}Tl in parathyroid localization. This may be partly due to a higher target-to-background ratio, but also to the superior physical characteristics of ^{99m}Tc .

J Nucl Med 1992; 33:313-318

The accepted radionuclide method for imaging abnormal parathyroid tissue has been the combined use of [^{99m}Tc]pertechnetate and [^{201}Tl]thallous chloride (1,2). High sensitivity of localization of parathyroid adenomas has been reported from a number of centers, although others have reported lower success rates and indeed some centers have reported unacceptably low sensitivities. While some of the differences in reported sensitivity (3-6) can be explained in different patient referral patterns (7), variations of size of the gland under assessment (8) and differing imaging protocols (9), the explanation in other

cases is less clear. These problems have called into question the role of ^{201}Tl parathyroid imaging (10-12) and highlighted the need for an improved parathyroid imaging agent.

Thallium-201 has suboptimal physical properties for imaging with a gamma camera. Specifically, the energy of its radiation is lower than ideal and there is a relatively high radiation dose to the patient. Technetium-99m-sestamibi is a cationic complex introduced for myocardial perfusion and used as an alternative to ^{201}Tl . In a preliminary study, we reported that sestamibi can also be used for parathyroid imaging (13). The current study was carried out to extend these preliminary observations in a larger patient population and see whether ^{99m}Tc -sestamibi could be used as a substitute for ^{201}Tl -chloride in routine clinical practice. The study was also designed to see whether the agent had different uptake characteristics in parathyroid tissue from ^{201}Tl .

METHOD

All patients had suspected hyperparathyroidism based on elevated levels of serum calcium and either inappropriately high serum parathormone levels or clinical suggestion of hyperparathyroidism. In four patients, previous neck surgery had been performed (two patients with recurrent parathyroid carcinoma and two patients who had failed parathyroidectomy at another hospital).

Thyroid localization was achieved using oral [^{123}I]sodium iodide (Mallinckrodt, UK) and parathyroid localization with both [^{201}Tl]thallous chloride (Mallinckrodt, UK) and ^{99m}Tc -sestamibi (Dupont, UK). These imaging studies were carried out on the same day.

The preoperative studies were performed using ^{201}Tl and ^{99m}Tc -sestamibi injected intravenously shortly before the removal of the surgical tissue. Iodine-123 was not given since thyroid localization was unnecessary as the surgeon was directly visualizing the neck tissues. The study outlines are as follows.

Scanning Procedure for Preoperative Localization

The thyroid was localized using oral [^{123}I]iodide (20 MBq) administered 4 hr before imaging. This was chosen rather than [^{99m}Tc]pertechnetate since its administration 4 hr before ^{201}Tl and ^{99m}Tc -sestamibi provided a stable count rate over the thyroid.

Received Sept. 6, 1991; revision accepted Oct. 3, 1991.
For reprints contact: Dr M.J. O'Doherty, Department of Nuclear Medicine,
Kent and Canterbury Hospital, Canterbury, Kent, U.K.

This was essential to allow the dynamic studies with both ^{201}Tl and to $^{99\text{m}}\text{Tc}$ -sestamibi to be carried out without changes in the count rate from the thyroid localizing agent.

Prior to imaging, a butterfly cannula was inserted into a large vein. The patient then laid supine with the head supported by a molded rest to avoid movement, and a pad under the shoulders was used to extend the neck. An anterior 300-sec image of the thyroid was obtained using a pinhole collimator and a 20% energy window for the 159 keV gamma emitted by ^{123}I . Following this, a 300-sec scatter image was acquired with a 20% energy window centered on 66 keV, corresponding to the energy of ^{201}Tl X-radiation. Taking care to avoid patient movement, 75 MBq of thallous chloride (^{201}Tl) were injected, followed by dynamic acquisition of 10, 120-sec frame times for 20 min. A 300-sec scatter image was then acquired using a 20% energy window centered on the 140 keV peak, corresponding to the $^{99\text{m}}\text{Tc}$ photopeak. A dose of 200 MBq of $^{99\text{m}}\text{Tc}$ -sestamibi was injected and a further ten, 120-sec time frames were acquired. The subsequent processing of these images included scatter correction of the thallium image from the iodine scatter image and $^{99\text{m}}\text{Tc}$ -sestamibi images from the iodine and thallium scatter image. A ^{201}Tl image consisting of the summation of the second to the tenth frame, an ^{123}I image and a subtracted image (^{123}I subtracted from the ^{201}Tl) were presented as hardcopy and an additional ^{123}I image, sestamibi image (summation of the second to the tenth frame) and a subtracted image (^{123}I subtracted from the $^{99\text{m}}\text{Tc}$ -sestamibi image) on separate hardcopy. Regions of interest were drawn around the thyroid tissue and superimposed on each frame of the dynamic acquisition to check for patient movement. If movement was detected, images were realigned with reference to the ^{123}I thyroid image. The scans were reported by two experienced observers.

In six patients who had discrete adenomas (ectopic or separate from the underlying thyroid), separate scatter-corrected time-activity curves were generated to demonstrate uptake of ^{201}Tl and $^{99\text{m}}\text{Tc}$ -sestamibi over the parathyroid and thyroid tissue. These time-activity curves were generated from a region of interest drawn over the parathyroid tissue and over the thyroid. Each point on these curves was normalized to the peak activity and expressed as a percentage of the peak.

Preoperative Study

Consecutive patients who were referred for surgery were studied, 13 with adenomas and 7 with hyperplasia. Parathyroid tissue was obtained from all of these patients. Thyroid tissue was obtained from all patients, but only those which were subsequently histologically normal were included for analysis. Technetium-99m-sestamibi (10 MBq) and 10 MBq of ^{201}Tl were administered to each patient in the operating theatre prior to removal of their parathyroid glands. Administered activities were measured from the difference between the syringe activity before and after injection. The time of injection was noted and the order of injection alternated between patients in case there was an effect of one tracer on the other in the circulation. The times of removal were taken to be the times of interruption of the blood supply to each gland. The injections were timed so that each patient's parathyroid tissue was removed after a different elapsed time following the administration of the radiopharmaceuticals. The tissue removed was weighed and the activity present in the parathyroid and thyroid tissue was measured using a re-entrant 7.5-cm diameter sodium iodide crystal (N.E. Technology, U.K.), calibrated for ^{201}Tl and $^{99\text{m}}\text{Tc}$ at a low activity level with an

TABLE 1
Adenomas Proven at Surgery (40 Patients) and Hyperplasia Proven at Surgery in 15 Patients (60 Glands)

	True-Positive	False-Negative
Scan findings for adenomas		
^{201}Tl	37	3
$^{99\text{m}}\text{Tc}$ -sestamibi	39	1
Scan findings for hyperplasias		
^{201}Tl	29	31
$^{99\text{m}}\text{Tc}$ -sestamibi	32	28

appropriate correction for crosstalk. The activities within the parathyroid and the thyroid were then expressed as Bq/MBq (tissue activity/injected activity).

RESULTS

Scans were performed in 57 patients undergoing surgical exploration. Forty patients have had confirmed adenomas, 15 with confirmed hyperplasia (8 with underlying renal failure), and 2 patients had parathyroid carcinomas with recurrences shown on reoperation. The two carcinoma patients, however, are not included in the analysis.

The scan findings for the patients with confirmed adenomas and confirmed hyperplasia are shown in Table 1. There was no apparent difference between the number of hyperplastic glands detected in the group with renal failure and the other patients and therefore only the total is shown. An example of the various scan appearances are shown in Figures 1–4. Figure 1 shows the scan appearances where both agents were taken up equally well. Figure 2 shows the different uptake between ^{201}Tl and $^{99\text{m}}\text{Tc}$ -sestamibi in an adenoma lying above the isthmus of the thyroid only seen with the $^{99\text{m}}\text{Tc}$ -sestamibi. Figure 3 is a scan where both agents failed to localize an adenoma weighing 2 g at the right lower pole of the thyroid. Figure 4 illustrates the slight differences noted in the visualization of hyperplastic tissue.

The dynamic curves for ^{201}Tl and $^{99\text{m}}\text{Tc}$ -sestamibi uptake in the thyroid and parathyroid tissue are shown in Figure 5. These data show that the uptake appears to peak at 4–6 min in both the thyroid and the parathyroid ade-



FIGURE 1. An ^{123}I thyroid image and a ^{201}Tl and $^{99\text{m}}\text{Tc}$ -sestamibi parathyroid image. The adenoma is clearly seen on both the ^{201}Tl and $^{99\text{m}}\text{Tc}$ -sestamibi images in the left lobe of the thyroid.



FIGURE 2. An ^{123}I thyroid image and a ^{201}Tl and $^{99\text{m}}\text{Tc}$ -sestamibi parathyroid image. The adenoma is clearly seen on the $^{99\text{m}}\text{Tc}$ -sestamibi scan and not on the ^{201}Tl in the region of the isthmus on the left side.

noma. The $^{99\text{m}}\text{Tc}$ -sestamibi activity in the parathyroid tissue remains relatively constant following the peak activity, whereas the ^{201}Tl activity steadily declines. Activity over the thyroid falls with both tracers.

The biopsy data for the 13 patients with resected adenomas and the 7 patients with resected hyperplastic glands are presented in Figures 6–9. Figure 6 illustrates that the uptake ratio of $^{99\text{m}}\text{Tc}$ -sestamibi to thallium in the three tissue types is variable. The mean \pm standard error of the mean (s.e.m.) of the thyroid tissue is 0.66 (0.04), for hyperplasia 0.77 (0.04) and for adenomas 0.83 (0.08). The uptake ratios in the adenomatous and hyperplastic tissue is greater than the thyroid tissue ($p < 0.05$) but not significantly different to one another. The highest ratios were found between 15 and 27 min for the adenomas and after 30 min for hyperplastic glands.

The relationship between $^{99\text{m}}\text{Tc}$ -sestamibi and ^{201}Tl uptake per gram of tissue is shown in Figure 7. For hyperplastic tissue, adenomatous tissue and thyroid tissue, the uptake of ^{201}Tl appears higher than that for $^{99\text{m}}\text{Tc}$ -sestamibi. The mean (s.e.m.) for uptake Bq/MBq/g of tissue in the thyroid, hyperplasia and adenoma was 151(23.3), 153.7 (18.4), 241 (31.9) for $^{99\text{m}}\text{Tc}$ -sestamibi and 232.1 (36.5), 210 (29.3) and 304.4 (38.5) for ^{201}Tl . There was increased uptake of ^{201}Tl in all tissues compared with $^{99\text{m}}\text{Tc}$ -sestamibi ($p < 0.001$ thyroid; $p < 0.001$ hyperplasia; $p < 0.02$ adenomas). However, only $^{99\text{m}}\text{Tc}$ -sestamibi had an



FIGURE 3. An ^{123}I thyroid image and a ^{201}Tl and $^{99\text{m}}\text{Tc}$ -sestamibi image. No evidence of an adenoma on either scan. A 2-g adenoma was removed at surgery from the lower pole of the right lobe of the thyroid.



FIGURE 4. Upper images show scatter corrected ^{201}Tl and $^{99\text{m}}\text{Tc}$ -sestamibi distribution. Lower images are after thyroid subtraction (^{123}I image of normal thyroid not shown). Three of the enlarged hyperplastic glands are demonstrated with both radiopharmaceuticals.

increased uptake per gram of parathyroid tissue compared with the thyroid ($p < 0.05$), whereas ^{201}Tl uptake did not reach statistical significance.

The time course of each radionuclide is illustrated in Figure 8 and shows that in the biopsy data the uptake in the thyroid falls rapidly with both ^{201}Tl and $^{99\text{m}}\text{Tc}$ -sesta-

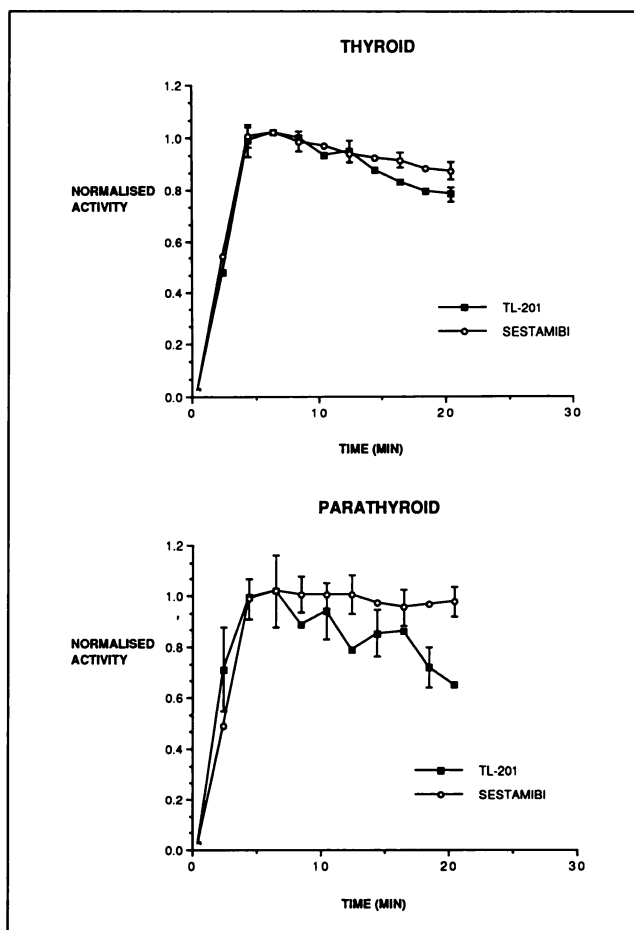


FIGURE 5. Dynamic time-activity curves for ^{201}Tl and $^{99\text{m}}\text{Tc}$ -sestamibi within regions of interest over thyroid and parathyroid tissue. The curves are normalized to the peak activity for each region and six thyroid regions and six parathyroid regions were used.

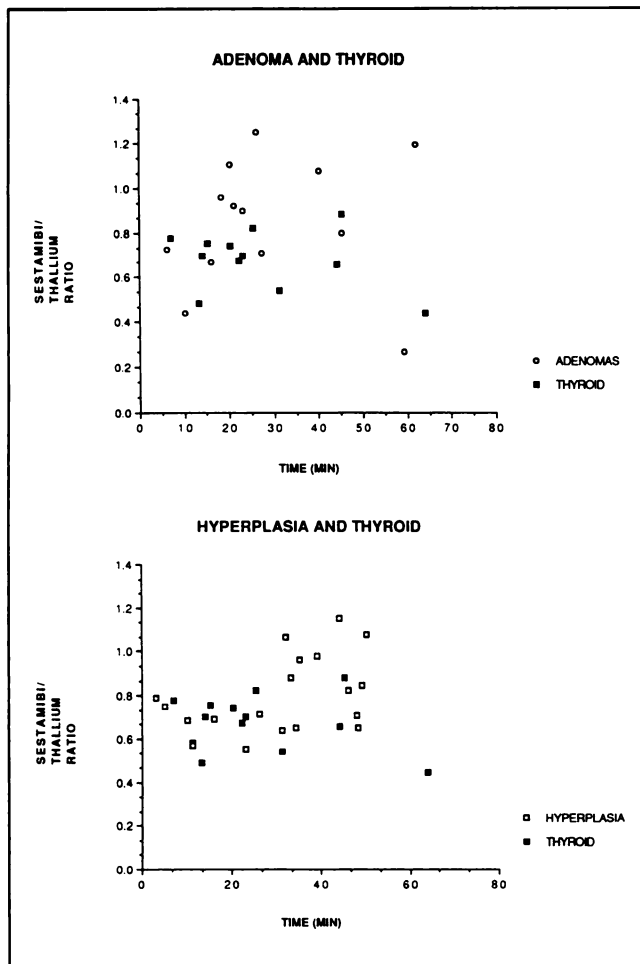


FIGURE 6. Uptake ratio for ^{99m}Tc sestamibi/ ^{201}Tl with time in adenomas (13), hyperplastic glands (21) and thyroid biopsies (12).

mibi. These data are from different patients and do not show any clear correlation of uptake of either ^{99m}Tc -sestamibi or ^{201}Tl with time. The ^{99m}Tc -sestamibi and ^{201}Tl uptake increased with the weight of hyperplastic and adenomatous tissue (Fig. 9). Adenoma tissue weight range was 0.194–5.020 g (mean 1.53 g); hyperplastic tissue range was 0.1–3.1 g (mean 0.88 g); and thyroid biopsies weighed 0.015–0.13 g (mean 0.038 g).

DISCUSSION

The sensitivity of our ^{201}Tl subtraction imaging for parathyroid adenomas (90%) compares favorably with our previous results with thallium imaging in adenomas (2) and other published studies (42%–96%) (7). For hyperplastic disease, our result was 47.5%, where sensitivities of 32%–100% have been reported (7,14). Because of our high sensitivity with ^{201}Tl subtraction imaging in adenomas, we have only demonstrated a small difference in detection rates with ^{99m}Tc -sestamibi to 98%, whereas with hyperplastic tissue the sensitivity improved to 55%. None of the

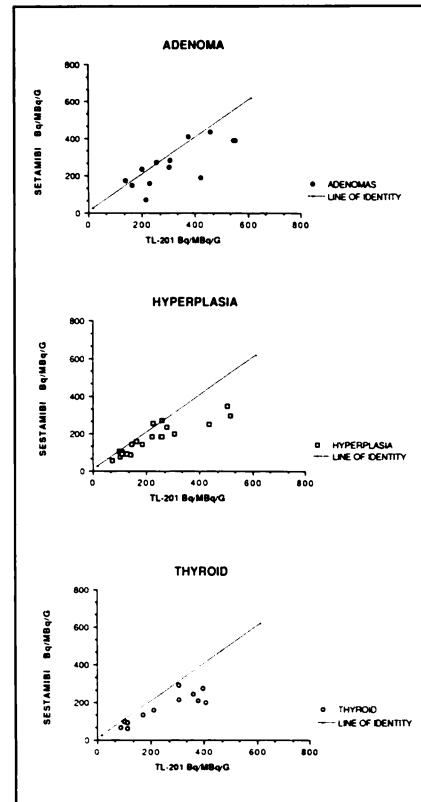


FIGURE 7. The relationship between ^{201}Tl and ^{99m}Tc -sestamibi uptake per gram of tissue in adenomas, hyperplasia, and thyroid.

true-positive ^{201}Tl cases produced a false-negative ^{99m}Tc -sestamibi-scan. This marginal improvement with ^{99m}Tc -sestamibi may be explained by the better imaging characteristics of ^{99m}Tc compared with ^{201}Tl and/or a difference in parathyroid uptake of ^{99m}Tc -sestamibi. The other factor which has probably played a role is the higher injected activity of ^{99m}Tc -sestamibi compared with ^{201}Tl .

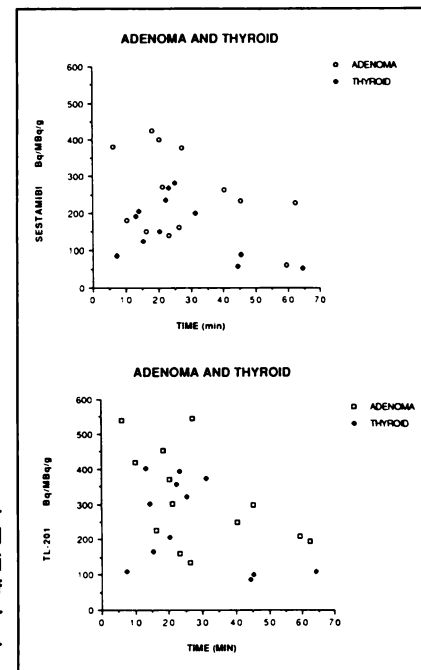


FIGURE 8. The relationship of ^{201}Tl and ^{99m}Tc -sestamibi uptake per gram of tissue with time for adenomas and thyroid tissue.

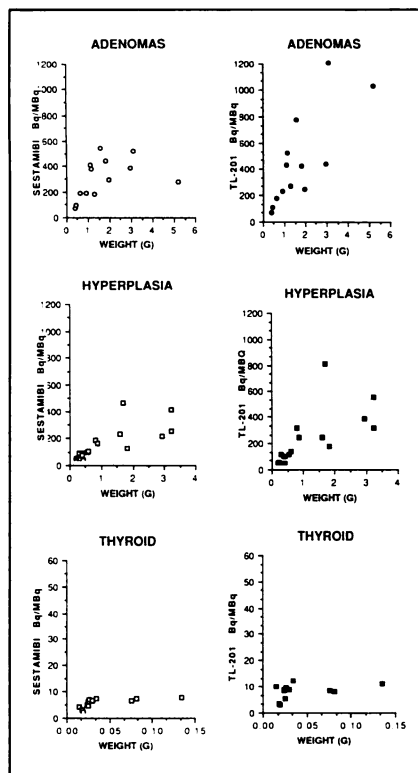


FIGURE 9. The relationship of ^{201}Tl and $^{99\text{m}}\text{Tc}$ -sestamibi activity with the weight of adenomatous, hyperplastic, and thyroid tissues.

The ^{201}Tl dose could not be increased because of the dosimetric considerations and the $^{99\text{m}}\text{Tc}$ -sestamibi dose was chosen to ensure an adequate count rate over the thyroid. Although in this current study we have not seen any false-positive results, this was due to the fact that there were no thyroid adenomas. Our previous report (13) demonstrated that thyroid adenomas will take up $^{99\text{m}}\text{Tc}$ -sestamibi, and, as with ^{201}Tl , we expect false-positive identification when these are present.

Localization of $^{99\text{m}}\text{Tc}$ -sestamibi in tissue will be dependent not only on the size of the gland but also on blood flow to the tissue, the concentration of $^{99\text{m}}\text{Tc}$ -sestamibi presented to the tissue and the binding mechanisms in various tissues.

Chiu et al. (15) have suggested that $^{99\text{m}}\text{Tc}$ -sestamibi is sequestered within the cytoplasm and mitochondria of mouse fibroblasts in response to the electrical potentials generated across the membrane bilayers of both the cell and the mitochondria. This suggests that a tissue with a large number of mitochondria may take up sestamibi more avidly than one with less. A difference in washout between sestamibi and thallium is seen in cardiac tissue (16), which has a large number of mitochondria per cell, with a longer retention of sestamibi. Recently, Sandrock et al. (17) showed that parathyroid adenomas had a large number of mitochondria in their cells and it is therefore possible that the $^{99\text{m}}\text{Tc}$ -sestamibi would be taken up more avidly in adenomatous tissue than the surrounding thyroid and following uptake a slower release would occur from the parathyroid cell.

The dynamic uptake data shows that in thyroid tissue there is a similar peak time of uptake with both agents and that they are released at a similar rate, whereas in the parathyroid adenomas the peak uptake still appears to be 4–6 min after injection, but there is slower release of sestamibi compared with thallium (Fig. 5). This would be consistent with a different turnover process within the glands and may be explained by the large number of mitochondria present. These data suggest that the maximum difference would be observed between thyroid and parathyroid tissue after 15 min.

The preoperative studies provide further evidence of differences between $^{99\text{m}}\text{Tc}$ -sestamibi and ^{201}Tl . Although the mean uptake of ^{201}Tl was greater than $^{99\text{m}}\text{Tc}$ -sestamibi in each tissue, no statistical difference in uptake could be demonstrated between ^{201}Tl in the parathyroid adenoma and the thyroid, whereas there was a difference observed with $^{99\text{m}}\text{Tc}$ -sestamibi in these tissues. This would suggest that the localization would be superior with $^{99\text{m}}\text{Tc}$ -sestamibi because of the higher target-to-background ratio.

There are a number of possible explanations why the mean uptake of ^{201}Tl is higher for both the parathyroid and thyroid tissues. It is possible the amount of ^{201}Tl available for uptake in the circulation may be greater than $^{99\text{m}}\text{Tc}$ -sestamibi. This is unlikely since both radiopharmaceuticals have similar half-time clearances from the blood (18,19). However a difference has been demonstrated in the first-pass extraction of thallium compared to sestamibi in the rabbit heart (16). In the heart, the first-pass peak extraction rates of sestamibi were only 30%–40% of the thallium values. This high first-pass extraction rate is offset later by the lower cell residence time of thallium compared to sestamibi.

In distinguishing the parathyroid tissue from underlying thyroid tissue, the most important factor is likely to be the quantity of tracer in each tissue. This difference in uptake is most marked between 15 and 28 min, when it can also be seen that the sestamibi/thallium ratio is greater than one (Fig. 6). These data suggest that there are slight biological differences between $^{99\text{m}}\text{Tc}$ -sestamibi and ^{201}Tl not only in the parathyroid but also the thyroid. This factor and the better physical imaging characteristics of the $^{99\text{m}}\text{Tc}$ compound should allow smaller gland localization with sestamibi. Gimlette et al. (8) predicted that the minimum gland size for parathyroid localization with ^{201}Tl would be 0.3 g, assuming a mean %uptake of the ID/g of parathyroid tissue 0.018%/g (range measured 0.011%–0.033%/g), our mean %uptake was 0.03%/g for adenomas and 0.021%/g for hyperplasia which agrees with these previous observations. However, the smallest gland in our current study was 0.194 g, which was detected using both $^{99\text{m}}\text{Tc}$ -sestamibi and ^{201}Tl .

A further consideration is the radiation dosimetry to the patient (Table 2). The calculated effective dose equivalent (EDE) data show that a radiation dose/MBq was 0.33 mSv/MBq for ^{201}Tl and 0.012 mSv/MBq for $^{99\text{m}}\text{Tc}$ -sesta-

TABLE 2
Dosimetry of Parathyroid Imaging

Radiopharmaceutical	Activity (MBq)	EDE (mSv)
^{99m} Tc]pertechnetate	75	1.0
¹²³ I	20	3.0
^{99m} Tc-sestamibi	200	2.4 (males) 3.0 (females)
²⁰¹ Tl	75	25

mibi. Using our study doses (200 MBq of ^{99m}Tc-sestamibi and 75 MBq of ²⁰¹Tl), there was a ten-fold reduction by using ^{99m}Tc-sestamibi in comparison with ²⁰¹Tl for parathyroid imaging. The use of ¹²³I is not essential for thyroid localization and was used in this study primarily to provide a constant thyroid background against which the dynamic ²⁰¹Tl and ^{99m}Tc-sestamibi data could be compared. Technetium-99m-pertechnetate has been used to provide the thyroid (20) image and its use with sestamibi should be further explored. The better imaging characteristics of ^{99m}Tc-sestamibi than ²⁰¹Tl and the relatively higher uptake in the adenomatous glands compared to the thyroid have also allowed tomography of adenomas (20) and may therefore provide an advantage in ectopic gland localization. Subjectively, our technologists have also found image processing to be slightly easier with ^{99m}Tc-sestamibi because the images contain less scatter.

It was concluded that ^{99m}Tc-sestamibi is selectively taken up by parathyroid adenomas compared to thyroid tissue and is at least equivalent to and perhaps superior to ²⁰¹Tl for localization of both adenomas and hyperplastic tissue. The factors associated with the superior physical characteristics of ^{99m}Tc-sestamibi compared with ²⁰¹Tl in terms of imaging and the smaller radiation dose to patients suggest that ^{99m}Tc-sestamibi is the more appropriate agent for imaging parathyroid tissue.

ACKNOWLEDGMENT

The authors would like to thank DuPont, UK for providing the sestamibi used in this study.

REFERENCES

1. Ferlin G, Borsato N, Perelli R. New perspectives in localizing enlarged parathyroids by technetium-thallium subtraction scan. *J Nucl Med* 1983;24:438-441.
2. Young AE, Gaunt JI, Croft DN, et al. Location of parathyroid adenomas by thallium-201 and technetium-99m subtraction scanning. *Br Med J* 1983;286:1384-1386.
3. Corcoran MO, Seifacian MA, George SL, Milroy SE. Localisation of parathyroid adenomas by thallium-201 and technetium-99m subtraction scanning. *Br Med J* 1983;286:1751-1752.
4. Miller DL, Doppman JL, Shawker TH, et al. Localisation of parathyroid adenomas in patients who have undergone surgery. 1. Noninvasive imaging methods. *Radiology* 1987;136:133-137.
5. MacFarlane SD, Hanelin LG, Taft DA, Ryan JA Jr, Fredlund PN. Localisation of abnormal parathyroid glands using thallium-201. *Am J Surg* 1984;148:7-12.
6. Okerlund MD, Sheldon K, Corpuz S, et al. A new method with high sensitivity and specificity for localization of abnormal parathyroid glands. *Ann Surg* 1984;200:381-388.
7. Sandrock D, Merino MJ, Norton JA, Neumann RD. Parathyroid imaging by Tc/Tl scintigraphy. *Eur J Nucl Med* 1990;16:607-613.
8. Gimlette TMD, Brownless SM, Taylor WH, Shields R, Simkin EP. Limits to parathyroid imaging with thallium-201 confirmed by tissue uptake and phantom studies. *J Nucl Med* 1986;27:1262-1265.
9. Fogelman I, McKillop JH, Bessent RG, et al. Successful localisation of parathyroid adenomata by thallium-201 and technetium-99m subtraction scintigraphy: description of an improved technique. *Eur J Nucl Med* 1984;9:545-547.
10. Goris ML, Basso LV, Keeling C. Parathyroid imaging. *J Nucl Med* 1991;32:887-889.
11. Consensus Development Conference Panel. Diagnosis and management of asymptomatic primary hyperparathyroidism: consensus development conference statement. *Ann Intern Med* 1991;114:593-597.
12. Coakley AJ. Parathyroid imaging—how and when. *Eur J Nucl Med* 1991;18:151-152.
13. Coakley AJ, Kettle AG, Wells CP, O'Doherty MJ, Collings REC. ^{99m}Tc-sestamibi—a new agent for parathyroid imaging. *Nucl Med Commun* 1989;10:791-794.
14. Wheeler MH, Harrison BJ, French AP, Leack KG. Preliminary results of thallium-201 and technetium-99m subtraction scanning of parathyroid glands. *Surgery* 1984;96:1078-1081.
15. Chiu ML, Kronange JF, Pivnicka-Worms D. Effect of mitochondrial and plasma-membrane potentials on accumulation of hexakis (2-methoxyisobutylisonitrile) technetium in cultured mouse fibroblasts. *J Nucl Med* 1990;31:1646-1653.
16. Meerdink DJ, Leppo JA. Comparison of hypoxia and ouabain effects on the myocardial uptake kinetics of technetium-99m hexakis 2-methoxyisobutyl isonitrile and thallium-201. *J Nucl Med* 1989;30:1500-1506.
17. Sandrock D, Merino MJ, Norton JA, Benton CS, Miller DL, Neumann RD. Light- and electron-microscopic analyses of parathyroid tumours explain results of Tl-201/Tc-99m parathyroid scintigraphy [Abstract]. *Eur J Nucl Med* 1989;15:410.
18. Wackers FJTh, Berman DS, Maddahi J, et al. Technetium-99m hexakis 2-methoxyisobutyl isonitrile: human biodistribution, dosimetry, safety, and preliminary comparison to thallium-201 for myocardial perfusion imaging. *J Nucl Med* 1989;30:301-311.
19. Atkins HL, Budinger TF, Lebowitz E, et al. Thallium-201 for medical use. Part 3: human distribution and physical imaging properties. *J Nucl Med* 1977;18:133-140.
20. Carroll MJ, Solanki KK, Britton KE, Besser GM. Change detection and movement correction for parathyroid imaging with Tc-99m MIBI [Abstract]. *J Nucl Med* 1991;32:1011.